Scaling of the bulk polarization in extended and localized phases of a quasiperiodic model

Balázs Hetényi
MTA-BME Quantum Dynamics and Correlations Research Group, Department of Physics, Budapest University of Technology and Economics, H-1111 Budapest, Hungary
and Institute for Solid State Physics and Optics, Wigner Research Centre for Physics, H-1525 Budapest, P. O. Box 49, Hungary

(Received 10 February 2024; revised 22 July 2024; accepted 29 August 2024; published 11 September 2024)

We study the finite size scaling of the bulk polarization in a quasiperiodic (Aubry-André) model using the geometric analog of the Binder cumulant. As a proof of concept, we show that the geometric Binder cumulant method described here can reproduce the known literature values for the flat and raised cosine distributions, which are the two distributions that occur in the delocalized phase. For the Aubry-André model at half-filling, the phase transition point is accurately reproduced. Not only is the correct size scaling exponent of the variance obtained in the extended and the localized phases, but the geometric Binder cumulant undergoes a sign change at the phase transition. We also calculate the state resolved Binder cumulant as a function of disorder strength to gain insight into the mechanism of the localization transition.

DOI: 10.1103/PhysRevB.110.125124

I. INTRODUCTION

The modern polarization theory [1–5] (MPT) overcomes the problem of the ill-defined nature of the position operator in systems with periodic boundary conditions (PBC) by casting crystalline polarization as a geometric or Berry [6] phase. In band insulators, polarization is an open path [7] geometric phase (also known as a Zak phase), while in many-body systems [8] it is a single-point geometric phase [4], the phase of the expectation value of a unitary operator. It is also possible to access moments and cumulants of the polarization [9,10]. The Zak phase can be viewed as the first member of a cumulant series. Gauge invariant cumulants [9] characterize band insulators, while the variance of the polarization, as derived [10] by Resta and Sorella (RS), provides a criterion for distinguishing [11] localized systems from extended ones. MPT is also the starting point [12,13] for deriving the characteristic invariants of topological insulators. Moments of the polarization form the backbone of maximally localized Wannier functions [14,15].

In the study of phase transitions, finite size scaling [16–20] is a useful tool. The finite systems accessible in calculations provide the expectation values of physical quantities (for example the magnetization in the Ising model), as well as their moments and cumulants, but care must be taken when extrapolating to the thermodynamic limit. Using the finite size scaling hypothesis [17,18], one can calculate the Binder cumulant [19,20] (BC). BC is a ratio of statistical cumulants of the order parameter (represented in quantum systems by an operator) useful in locating critical points. BC is equivalent to the *excess kurtosis* [21] (EK) of the order parameter, a quantity widely used in probability and statistics to characterize the tail and peak of probability distributions. An EK of zero corresponds to a Gaussian distribution, while a distribution with positive(negative) EK is referred to as super-Gaussian(sub-Gaussian). In MPT, the polarization is not an expectation value of an operator, it is a geometric phase, so it is not immediately obvious whether a BC can be constructed for the polarization in crystalline systems.

MPT, in its original form, does not provide accurate finite size scaling information in the delocalized phase. For disordered systems [22,23] or in many-body localization studies [24,25], the inverse participation ratio is used instead of MPT, even though MPT was developed to address the localization of charge carriers. Kerala Varma and Pilati [26] made a thorough investigation of RS in quasiperiodic models. They find some disagreement in the behavior of the variance between open boundary conditions (OBC) and PBC. RS can be interpreted as a second cumulant (variance) obtained from a particular generating function. It is possible to extend to RS formalism to derive higher order cumulants as well [27,28] but these diverge in metallic phases and it is not possible to construct a BC. Recently an alternative approximation scheme [27,28], which preserves the scaling information of the variance in the metallic, as well as the insulating phases, was suggested to circumvent these problems. Since the approach amounts to formulating a Binder cumulant in the context of a geometric phase, the method will be named the geometric Binder cumulant (GBC).

In this work, we apply the GBC to the Aubry-André [29] (AA) model. The AA model is used to study quasicrystals [30–32] and the localization phenomenon [33–37]. It exhibits a phase transition between extended and localized states at a finite on-site potential potential strength. At finite system size we find that the ground state on the metallic side can be degenerate. We discuss ways to handle this issue. The distribution function of the polarization in the degenerate case is a raised cosine distribution (RCD), whose EK is a specific number known from the statistics literature [38]. Our lowest order approximation does not reproduce that known value, but as higher order finite difference approximations are used the fourth order GBC (U_4) converges to it (Fig. 1). The GBC also characterizes the critical exponents near the AA transition and locates the transition point accurately (Figs. 3 and 4).

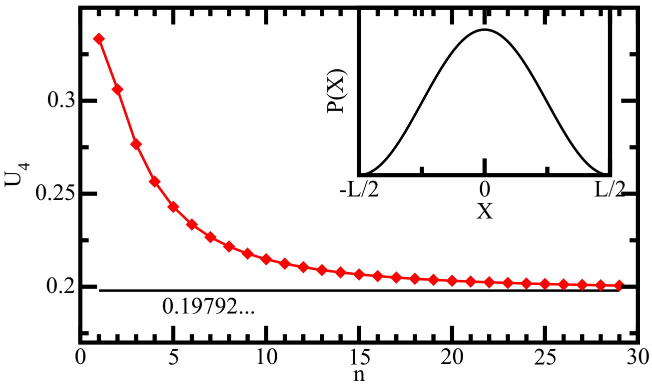

FIG. 1. Binder cumulant for a closed gap system with a twofold degenerate ground state as a function of n. The value of n determines the order of the finite difference approximation ($\mathcal{O}(L^{-2n})$). As the approximation is improved, the geometric Binder cumulant approaches the limiting value of 0.19792... which corresponds to the known [38] value of the excess kurtosis for the raised cosine distribution.

We also calculate the GBC for individual eigenstates (Fig. 5) and find that all states are delocalized in the extended phase, while in the localized phase, only *some* states become localized, but this causes the entire system (at half-filling) to localize at finite fillings. For the AA model Jitomirskaya [34] has shown that for infinite systems all states localize at the transition point ($W = 2t$). Recently this result was questioned to some extent by the suggestion [36,37] of "almost localized" states. Our results within periodic boundary conditions suggest that some states remain delocalized even for $W > 2t$, but this may be due to the periodic boundary conditions. It is to be noted that a calculation of this type is not possible without the use of the technique developed here: our technique allows the determination of whether a state is localized or not from one calculation on the state itself, without having to compare different system sizes.

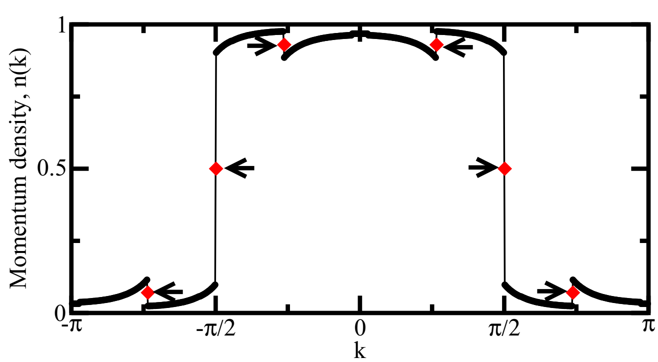

FIG. 2. Momentum density [44] as a function of k across the Brillouin zone for an Aubry-André model with 610 lattice sites for $t = W = 1$ (extended phase). The momentum density has discontinuities as a function of k, at $k = \pm\frac{\pi}{4}, \pm\frac{\pi}{2}, \pm\frac{3\pi}{4}$. Filled black circles indicate a system with Peierls phase $\phi = 0$, while the red diamonds indicate the states that appear when a Peierls phase of $\phi = \pi/L$ is applied to shift the momenta of states. These extra states, which always appear halfway through discontinuities are indicated by six arrows.

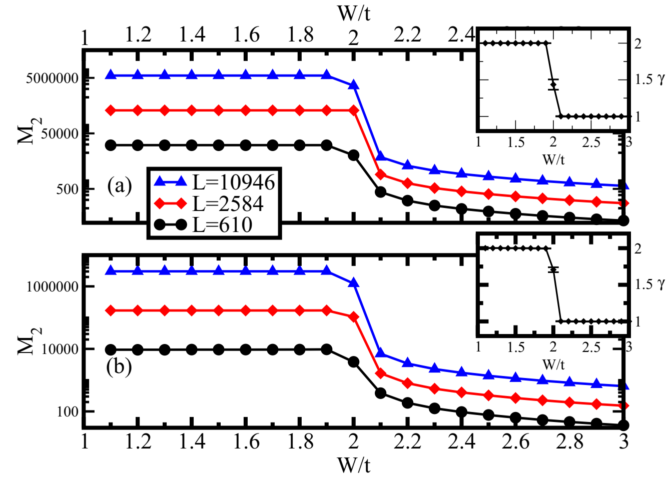

FIG. 3. (a) M_2 (second cumulant) as a function of W/t for system sizes $L = 610,\ 2584,$ and 10 946. For $L = 610$ and 10 946, $\phi = 0$ (corresponding to periodic boundary conditions), while for $L = 2584$, $\phi = \pi/L$ (corresponding to antiperiodic boundary conditions). The ground state in all three cases is nondegenerate. (b) same as (a) except the Peierls phase is $\phi = \pi/L$ for $L = 610$ and 10 946, and $\phi = 0$ for $L = 2584$. The ground state in all three cases is degenerate.

Our paper is organized as follows. In the next section, the MPT based cumulant method is assembled. In Sec. III, the model and the specificities of the calculation are chronicled. We then relate a Widom scaling analysis, in which we derive and then numerically verify a universal relation between critical exponents. In Sec. V, we address the effects of ground state degeneracy. In Sec. VI, the results of our calculations are presented. In Sec. VII, we conclude our work.

II. GEOMETRIC BINDER CUMULANT

In this section we construct a version of the Binder cumulants adapted to the context of the modern polarization theory (MPT), which we will refer to as the geometric Binder

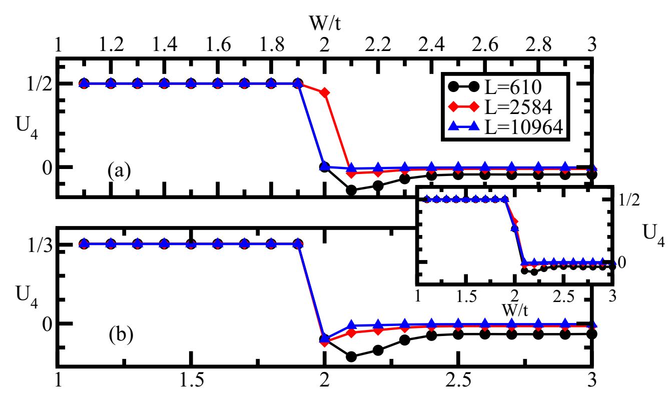

FIG. 4. (a) U_4 (geometric Binder cumulant) as a function of W/t for system sizes $L = 610,\ 2584,$ and 10 964 for the case with a nondegenerate ground state. (b) same as (a) but for the case with a degenerate ground state. The inset shows the same systems as (b) but with U_4 calculated via a two grid-point approximation.

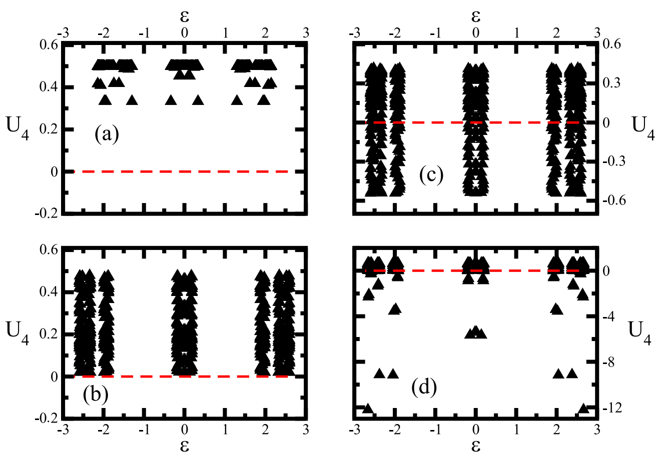

FIG. 5. Geometric Binder cumulant U_4 of a a given energy eigenstate as a function of energy eigenvalue of the Aubry-André model for different values of W/t: (a) 1.00, (b) 1.99, (c) 2.01, and (d) 2.10. The red dashed line indicates $U_4 = 0$.

cumulant (GBC). We briefly introduce the MPT by way of the twist operator, and then focus on how cumulants are constructed. Moments and cumulants are derivatives of the generating function, but in a periodic system this function is only defined on a discrete set of k-points, so one can not take an exact derivative. Given that, the usual approach is to take finite difference derivatives, and we argue that it is crucial how the finite difference approximation is applied, because not all approximation schemes can reproduce finite size scaling information. Our approach is validated through the reproduction of the known value of the excess kurtosis for a number of distribution functions (Fig. 1 of Ref. [28] and Fig. 1 of this work) found in the delocalized phase. As for the insulating phase, it was shown [28] that the GBC (U_4) can only take nonzero values for adiabatic paths which cross degeneracy points, and it is always zero for fully adiabatic paths. Based on this one can expect that in the insulating phase the GBC always takes a value of zero. Our numerical results show that this happens in the limit of large system sizes. A GBC of zero corresponds to a Gaussian distribution of the polarization.

A. Twist operator

In MPT, the position operator is not used directly. Instead, for the electronic contribution [39] of the polarization, expectation values of the twist operator,

$$\hat{U} = \exp\left(i\frac{2\pi}{L}\hat{X}\right), \tag{1}$$

are taken, from which the total position and its cumulants can be extracted. In Eq. (1), L is the length of the system in which it is periodic, $\hat{X} = \sum_{j=1}^{N} x_j \hat{n}_j$ is the total position operator (x_j denotes the position, $\hat{n}_j$ denotes the density operator at site j, and N is the number of particles). The expectation value over some ground state Ψ,

$$Z_q = \langle\Psi|\hat{U}^q|\Psi\rangle \tag{2}$$

can be interpreted as a characteristic (cumulant generating) function, associated with the probability distribution of the total position,

$$P(X) = \langle\Psi|\delta(X - \hat{X})|\Psi\rangle. \tag{3}$$

Since $P(X)$ is periodic in L, Z_q is only defined on a discrete set of points $q = 0, \ldots, L-1$. In general, Ψ denotes a correlated ground state. In band systems, such as the Aubry-André model we study, Ψ is a Slater determinant constructed from occupied Bloch states.

B. Cumulants in statistics

Given a normalized probability distribution function, $P_0(x)$, which satisfies

$$P_0(x) \geqslant 0, \int_{-\infty}^{\infty} dx P_0(x) = 1, \tag{4}$$

one can define the associated characteristic function,

$$f(k) = \int_{-\infty}^{\infty} dx \exp(ikx) P_0(x). \tag{5}$$

The nth moment (M_n) and the nth cumulant (C_n) of $P(x)$ can be obtained from $f(k)$ as

$$M_n = \frac{1}{i^n}\frac{\partial^n f(k)}{\partial k^n}\bigg|_{k=0} = \langle x^n\rangle,$$
$$C_n = \frac{1}{i^n}\frac{\partial^n \ln f(k)}{\partial k^n}\bigg|_{k=0}, \tag{6}$$

where $\langle\rangle$ denote the average over $P_0(x)$. The moments and cumulants are related to each other, the first few such relations can be written as

$$\begin{aligned} C_1 &= M_1, \quad C_2 = M_2 - M_1^2,\\ C_3 &= M_3 - 3M_2M_1^2 + 2M_1^3,\\ C_4 &= M_4 - 4M_3M_1 - 3M_2^2 + 12M_2M_1^2 - 6M_1^4. \end{aligned} \tag{7}$$

C_1 is known as the mean, C_2 is the variance, C_3 is the skew, and C_4 is the kurtosis. The distribution, $P(x)$ can be shifted so that the mean is zero. In this case, the cumulants and moments become centered, and the relations in Eq. (8) become

$$\begin{aligned} C_1 &= 0, \quad C_2 = M_2,\\ C_3 &= M_3, \quad C_4 = M_4 - 3M_2^2. \end{aligned} \tag{8}$$

The excess kurtosis, used in statistics to characterize the tails of distribution functions, is defined as,

$$K_E = \frac{C_4}{C_2^2}. \tag{9}$$

When the quantity x refers to the order parameter of a physical system, the fourth order Binder cumulant (U_4) is often used in finite size scaling,

$$U_4 = 1 - \frac{M_4}{3M_2^2} = -\frac{1}{3}K_E, \tag{10}$$

which is equivalent to the excess kurtosis. The two quantities only differ in the factor of $-\frac{1}{3}$.

C. Case of periodic probability distribution functions

In the modern theory of polarization, crystalline systems are treated, whose Hamiltonians are taken as periodic. The underlying probability distributions are also periodic. We can write

$$P(x) = \sum_{w=-\infty}^{\infty} P_0(x + wL), \tag{11}$$

where $P_0(x)$ is a normalized probability distribution, not periodic, as defined in Eq. (4). $P(x)$ is periodic in L. One is interested in the moments and cumulants of $P_0(x)$, but the characteristic function is only available at a discrete set of k points,

$$k_q = \frac{2\pi}{L} q, \tag{12}$$

where $q = 0, \dots, L-1$. This also means that the derivatives which need to be calculated to obtain C_n or M_n have to be approximate derivatives. Most often they are finite difference derivatives. Denoting the discrete characteristic function as Z_q, which we define as

$$Z_q = \int dx P_0(x) \exp\left(i\frac{2\pi}{L} qx\right). \tag{13}$$

The Resta-Sorella approximation for the variance amounts to using a finite difference approximation for C_2 of order $\mathcal{O}(L^{-2})$,

$$C_2 = \left(\frac{L}{2\pi i}\right)^2 (\ln Z_1 + \ln Z_{-1} - 2\ln Z_0) = -\frac{L^2}{2\pi^2} \ln|Z_1|. \tag{14}$$

In the last part of this equation, we used the fact that $Z_{-1} = Z_1^*$, and that $Z_0 = 1$.

D. Finite difference derivatives

Given a function $f(x)$ represented on a discrete set of points, $f_q = f(qh)$, with q integer, where h denotes the spacing between the points. One can construct [40] the centered finite difference approximation of f_q to different levels of accuracy. For example, for the second derivative at $q = 0$, we can write

$$\left.\frac{\partial^2 f(x)}{\partial x^2}\right|_{x=0} \approx \frac{f_1 + f_{-1} - 2f_0}{h^2}. \tag{15}$$

This approximation leads to an error of order $\mathcal{O}(h^{-2})$. The Resta-Sorella variance can be derived using this approximation, by associating $h = \frac{2\pi}{L}$ and $\ln|Z_q| = f_q$. One can also improve on the Resta-Sorella scheme, by using higher order approximations to the second derivative, for example, the next order ($\mathcal{O}(h^{-4})$) is

$$\left.\frac{\partial^2 f(x)}{\partial x^2}\right|_{x=0} \approx \frac{-f_2 + 16f_1 - 30f_0 + 16f_{-1} - f_{-2}}{12h^2}. \tag{16}$$

We see that in higher order approximations f_qs with larger qs appear. Using this approximation one can obtain an $\mathcal{O}(h^{-4})$ approximation to the variance,

$$C_2 = \frac{L^2}{24\pi^2}(\ln|Z_2| - 16\ln|Z_1|). \tag{17}$$

By including more Z_qs with larger qs one can obtain systematically improved approximations in the insulating phase.

It is also possible to derive higher order cumulants, such as the kurtosis, needed to construct the Binder cumulant. The lowest order ($\mathcal{O}(h^{-2})$) approximation to the fourth derivative reads as

$$\left.\frac{\partial^4 f(x)}{\partial x^4}\right|_{x=0} \approx \frac{f_2 - 4f_1 + 6f_0 - 4f_{-1} + f_{-2}}{h^4}. \tag{18}$$

Based on this approximation, one can write an expression for the kurtosis of the polarization as

$$C_4 = \frac{L^4}{8\pi^4}(\ln|Z_2| - 4\ln|Z_1|), \tag{19}$$

alternatively, using the next best approximation results in

$$C_4 = \frac{L^4}{48\pi^4}(-\ln|Z_3| + 12\ln|Z_2| - 39\ln|Z_1|). \tag{20}$$

Again, higher order approximations need Z_qs with progressively larger values of q. In principle, one is in a position now to construct the Binder cumulant, since both C_4 and C_2 are available. However, if one used the above approximations, one would encounter a problem, namely that the terms Z_q approach zero in the extended phase, leading to divergences in $\ln Z_q$.

E. Approximating the logarithm

It is, of course, possible to approximate the terms $\ln|Z_q|$, by expanding the quantity $(|Z_q| - 1)$, resulting in

$$\ln[1 + (|Z_q| - 1)] = (|Z_q| - 1) - \frac{(|Z_q| - 1)^2}{2} + \dots \tag{21}$$

Using this approximation in $\mathcal{O}(L^{-2})$ expressions for C_4 [Eq. (19)] and C_2 [Eq. (14)] lead to

$$\begin{aligned} C_2 &= \frac{L^2}{2\pi^2}(1 - |Z_1|), \\ C_4 &= \frac{L^4}{8\pi^4}(-|Z_2| + 4|Z_1| - 3). \end{aligned} \tag{22}$$

We define the geometric Binder cumulant (GBC) as

$$U_4 = -\frac{1}{3}\frac{C_4}{C_2^2}. \tag{23}$$

In the nondegenerate case of the extended phase all $Z_q \to 0$, except Z_0 which is unity. It follows that $U_4 = \frac{1}{2}$. In the degenerate case, as discussed below, $Z_q \to 0$, except for $Z_0 = 1$ and $Z_1 = 1/2$, leading to $U_4 = \frac{1}{3}$. In the extended state $\ln Z_q$ for $q > 1$ will diverge. C_2 will not diverge at $\mathcal{O}(L^{-2})$, but if higher order approximations are used, it will. Also C_4 will diverge, and so will U_4. This means that in the original RS scheme size scaling information in the extended phase will be lost. Approximating $\ln Z_q$ as in Eq. (21) solves this problem.

It may appear that the GBC technique advocated here is worse than the original RS scheme, since another approximation is introduced. It is to be noted that the two simple polarization distributions which occur in the extended phase (the flat distribution in the nondegenerate case, and the RCD in the degenerate case) both have known EK values, which are reproduced by the GBC technique (Fig. 1 in Ref. [28] and Fig. 1), but this can not done by the original RS scheme, which exhibits divergences.

III. MODEL AND CALCULATION DETAILS

We consider a Hamiltonian of the Aubry-André type given by

$$\hat{H} = -t\sum_{j=1}^{L}(c_{j+1}^{\dagger}c_j + c_j^{\dagger}c_{j+1}) + W\sum_{j=1}^{L}\xi_j n_j, \tag{24}$$

where $\xi_j = \cos(2\pi\alpha j)$, where α is the golden ratio obtained from the ratio of consecutive members of the Fibonacci sequence in the limiting case, and the operators $c_j^{\dagger}(c_j)$ create(annihilate) a particle at site j. For finite systems with PBC, the irrational α is approximated as a ratio $\alpha \approx F_{n+1}/F_n$, where F_n is the nth Fibonacci number, so the size of the system can not be smaller than F_n.

In our calculations below, we diagonalize $\hat{H}$ under periodic boundary conditions, meaning that we obtain a set of states on the lattice, $\Phi_\lambda(j)$, where λ denotes the state index, and j denotes the lattice site. For a system with N particles, the ground state wave function is a Slater determinant consisting of the N states, $\Phi_\lambda(j)$, $\lambda = 1, \ldots, N$ with lowest energy,

$$\Psi(j_1, \ldots, j_N) = \mathrm{Det}[\Phi_\lambda(j_\mu)], \tag{25}$$

where j_μ denotes the lattice coordinate of particle μ, and $\mu = 1, \ldots, N$. To calculate the quantity Z_q, one can use the fact that the overlap of determinants equals the determinant of overlaps, resulting in

$$Z_q = \langle\Psi|\hat{U}^q|\Psi\rangle = \mathrm{Det}[\langle\Phi_\lambda|\hat{u}^q|\Phi_{\lambda'}\rangle], \tag{26}$$

where $\hat{u}$ denotes the one-body analog of $\hat{U}$ resulting in

$$\langle\Phi_\lambda|\hat{U}^q|\Phi_{\lambda'}\rangle = \sum_{j=1}^{L}\phi_\lambda^*(j)\exp\left(i\frac{2\pi q}{L}j\right)\phi_{\lambda'}(j). \tag{27}$$

IV. WIDOM SCALING IN THE AUBRY-ANDRÉ MODEL

By considering the continuous generalization of Z_q, which occurs in the thermodynamic limit, it is possible to construct a scaling theory within the MPT. This was done in Ref. [41]. Sending $\frac{2\pi}{L}q \to K$, we define the singular "free energy" $\Phi(w, K) = \ln Z(w, K)$, where $w = \frac{W-W_c}{t}$ denotes the reduced potential strength in the vicinity of the transition ($W_c = 2$). The second and fourth cumulants (susceptibilities) all diverge as W_c is approached. Using the usual definition for susceptibilities,

$$\chi^{(n)} = \frac{1}{i^n}\frac{\partial^n\Phi(w, K)}{\partial K^n}, \tag{28}$$

one can define critical exponents which characterize the system in the vicinity of W_c,

$$\begin{aligned}\chi^{(2)}(w, 0) &\propto 1/w^{\beta},\\ \chi^{(4)}(w, 0) &\propto 1/w^{\alpha},\\ \chi^{(2)}(0, K) &\propto 1/K^{\delta}.\end{aligned} \tag{29}$$

Assuming the Widom scaling form, $\Phi(\lambda^a w, \lambda^b K) = \lambda\Phi(w, K)$ leads to the relation between the critical exponents,

$$\alpha\delta = \beta(\delta + 2). \tag{30}$$

In Ref. [41], the exponent δ was determined to be $\delta = 2$, since this exponent characterizes the system at the critical point, and the distribution of the extended state can be used to estimate it for any model with a localization transition. This results in the relation $\alpha = 2\beta$, which appears to be a universal relation in 1D systems for transitions accompanied by gap closure. For other 1D models, this relation was verified in Ref. [41]. Here, we also find verification for the AA model: we find $\alpha = 2$ and $\beta = 1$, in agreement with Eq. (30).

V. GROUND STATE DEGENERACY

In 1D lattice models, a degeneracy often occurs for finite systems, see, for example, Ref. [42,43]. The origin of this degeneracy is the fact that the Brillouin zone for a finite system is discrete, and whether it occurs or not depends on the parity of N and/or L. This effect is expected to disappear in the thermodynamic limit, and is therefore considered an artifact. Still, calculations are done in finite systems, so it is important to understand the effects of this degeneracy. In this section, we discuss how it effects the GBC, and also present various ways of addressing it.

In the extended state, we find that the GBC can take two values, $U_4 = \frac{1}{2}$ or $\frac{1}{3}$. The former(latter) corresponds to a nondegenerate(degenerate) ground state. In the nondegenerate case, all $Z_q = 0$, except, $Z_0 = 1$. When the ground state is degenerate, $Z_0 = 1$, $|Z_1| = 1/2$, and all other Z_q are zero. The degeneracy depends on the optimal spacing of k-vectors in the Brillouin zone and whether N and L are even or odd.

The quantity Z_q is a scalar product, $\langle\Psi|\tilde{\Psi}\rangle$, where $|\tilde{\Psi}\rangle = \exp(i\frac{2\pi q}{L}\hat{X})|\Psi\rangle$ denotes the ground state with all momenta shifted by $\frac{2\pi}{L}q$ as a result of the twist operator. If the ground state is nondegenerate, then there is only one ground state, which has to have zero total momentum. Since Z_q will be the scalar product of a zero momentum state and one with a finite momentum (due to the action of $\hat{U}^q$), all $Z_q = 0$, except if $q = 0$. When the ground state is degenerate, the ground state wave function will have two components, one with total momentum π/L, the other with total momentum $-\pi/L$. Let us write this ground state wave function as

$$|\Psi\rangle = a|\Psi_{\pi/L}\rangle + b|\Psi_{-\pi/L}\rangle, \tag{31}$$

where a and b are two complex numbers, each with magnitude $1/\sqrt{2}$, because the total wave function has to have zero total momentum. To calculate Z_1, we apply the shift operator $\hat{U}$ once, resulting in

$$|\tilde{\Psi}\rangle = \hat{U}|\Psi\rangle = a|\Psi_{3\pi/L}\rangle + b|\Psi_{\pi/L}\rangle. \tag{32}$$

Evaluating the scalar product results in

$$Z_1 = \langle\Psi|\tilde{\Psi}\rangle = a^*b, \tag{33}$$

from which it follows that $|Z_1| = 1/2$. A similar analysis shows that other $Z_q = 0$, except $Z_0 = 1$.

The momentum density [44] for both the degenerate and nondegenerate cases is shown in Fig. 2 in the extended phase indicating discontinuities. In the degenerate case, states are found with momentum density precisely at the discontinuity, indicated by arrows in the figure. The Fourier transform of Z_q gives the polarization distribution [Eq. (13)]. For a metallic system with a nondegenerate ground state this distribution is flat, while for a degenerate system it is RCD (inset of Fig. 1). For both functions the GBC (or EK) takes well-known values [38] ($U_4 = 0.4$ and $U_4 = 0.19792\ldots$, respectively). Our results based on Eqs. (22) and (23) do not coincide with those values, but if higher order approximations are used, our U_4s converge to the known values. For the nondegenerate case (flat distribution), this is shown in Fig. 1 of Ref. [28], for the degenerate case (RCD), we present it in Fig. 1 of this work.

The results of the above calculations suggest several ways to get around the degeneracy issue. One is to handle the two cases (degenerate and nondegenerate) separately, since in the former(latter), the GBC will tend to 1/3(1/2) in the extended phase. It is also possible to apply a Peierls phase of π/L to lift the degeneracy (or to generate a degenerate ground state). Such calculations are presented in Figs. 3 and 4. It is also possible to construct a U_4 which is not sensitive to this degeneracy. To do this, send $q \to 2q$ in all the Z_q's occurring Eq. (22), amounting to doubling the distance over which the finite difference derivative is defined. Results for a calculation of this type are shown in the inset of Fig. 4. As presented in the Results section, all of these methods work in locating the critical point.

For locating critical points, our results for AA below, and previous studies [27,28] show that U_4 approximated up to $\mathcal{O}(L^{-2})$ works well. The original RS variance [8,10] is based on a finite difference logarithmic derivative and it is correct up to $\mathcal{O}(L^{-2})$. It is possible to construct higher order cumulants to any order approximation by extending the RS scheme as well (see, for example, Eq. (51) of Ref. [28]), however, these will fail to give the known values of the flat or the RCD for the EK, because of terms like $\ln Z_q$ with $q > 0$ which diverge as $Z_q \to 0$.

VI. RESULTS

Figure 3 shows the second cumulant of the polarization as a function of W/t for both nondegenerate (a) and degenerate (b) ground states. Three system sizes, $L =$ 610, 2584, and 10 946, were investigated. Two sets of results are shown, the upper (lower) panel for a nondegenerate (degenerate) ground state. In the region $W/t < 2$, the functions are straight lines, a drastic change occurs at $W/t = 2$, the transition point. Defining the size scaling exponent γ as $M_2 = aL^\gamma$, we find that for $W/t < 2$, $\gamma = 2$, while for $W/t > 2$, $\gamma = 1$ (negligible error in both cases). These results are in line with expectations [45]. At the transition point itself, we find $\gamma = 1.44(7)$ [$\gamma = 1.71(3)$] for the nondegenerate (degenerate) case. The phase transition point is clearly identified. For comparison, Ref. [26] reports a flat variance and $\gamma = 2.008(5)$ for OBC, meaning that our method for PBC, in this sense, coincides with their OBC results.

The Binder cumulant results (Fig. 4) corroborate the findings based on the variance. In the regime of extended states, the Binder cumulant shows the predicted sensitivity to ground state degeneracy, because its value is 1/2 (1/3) for the nondegenerate (degenerate) case. In the localized regime the GBC becomes negative but tends to zero with both increasing disorder strength and system size.

Figure 4 shows that the transition can be determined using one system size only when U_4 is used, since even for one system size U_4 changes sign. We now exploit this feature to calculate localization in individual eigenstates of the AA model. To gain insight into the localization mechanism, we calculated U_4 for each eigenstate for different values of W/t (Fig. 5). For $W/t = 0$ (not shown), all states are extended ($U_4 = \frac{1}{2}$). The states are evenly distributed, no clustering occurs, there are no gaps. As W is increased, but still metallic, bands form, with gaps between them, clustering is seen in (a) and (b) of Fig. 5. While the values of U_4 span a wider range, all states have $U_4 > 0$. As the phase boundary is crossed, a fraction of states localize, $U_4 < 0$. Interestingly, not all states have $U_4 < 0$, some appear to remain delocalized, at least in the periodic box of size $L = 610$. Unlike in uncorrelated disordered systems [22] with mobility edges, the localized states are not necessarily on the edges of the bands. In the AA in 1D, at half-filling, the wave function is a Slater determinant of occupied states, the localized states localize the whole system. Away from half-filling the critical point remains $W/t = 2$. This follows from the results in Fig. 4.

VII. CONCLUSION

We developed a finite size scaling method to be used to locate quantum phase transition points in the context of the modern polarization theory, where the polarization is expressed as a geometric phase, rather than the expectation value of an operator. The method was applied to the Aubry-André model, the canonical model in the study of quasi-periodicity, and one which exhibits a transition between extended and localized phases. The Binder cumulant construction allows the determination of localization of individual states, because, unlike when the variance is used, a comparison between different system sizes is not necessary. We calculated the localization of individual eigenstates and found that some of the states remain delocalized even upon crossing the phase transition point. This result raises interesting questions about localization, and how it occurs [34,36,37] when periodic boundary conditions are used.

In a seminal paper in 1964, Walter Kohn [11] was the first to point out that the quantum criterion to distinguish conductors from insulators is the localization of the center of mass of the charge distribution, rather than the localization of individual charge carriers, which is the appropriate criterion in the classical case. The numerical testing of this idea was not possible at the time, because in model calculations periodic boundary conditions are used, and the position operator is ill-defined. The modern theory of polarization, developed [1,2] in the 1990s, overcame this problem by casting the polarization as a geometric phase [6,7]. All example calculations based on this theory support the original tenet of Kohn. Our work provides for the use of scaling methods [17–20], originating from renormalization group theory, in a modern polarization theoretical context, and allows for quantitative tests of Kohn's tenet.

ACKNOWLEDGMENTS

I thank M. V. Berry for helpful discussions. I was supported by the National Research, Development and Innovation Fund of Hungary within the Quantum Technology National Excellence Program (Project No. 2017-1.2.1-NKP-2017-00001) and by Grants No. K142179 and No. K142652 and by the BME-Nanotechnology FIKP Grant No. (BME FIKP-NAT).

[1] R. D. King-Smith and D. Vanderbilt, Theory of polarization of crystalline solids, Phys. Rev. B **47**, 1651 (1993).

[2] R. Resta, Macroscopic polarization in crystalline dielectrics: the geometric phase approach, Rev. Mod. Phys. **66**, 899 (1994).

[3] D. Vanderbilt, *Berry Phases in Electronic Structure Theory* (Cambridge University Press, Cambridge, UK, 2018).

[4] R. Resta, Manifestations of Berry's phase in molecules and condensed matter, J. Phys.: Condens. Matter **12**, R107 (2000).

[5] N. Spaldin, A beginner's guide to the modern theory of polarization, J. Solid State Chem. **195**, 2 (2012).

[6] M. V. Berry, Quantal phase factors accompanying adiabatic changes, Proc. R. Soc. London A **392**, 45 (1984).

[7] J. Zak, Berry's phase for energy bands in solids, Phys. Rev. Lett. **62**, 2747 (1989).

[8] R. Resta, Quantum mechanical position operators for extended systems, Phys. Rev. Lett. **80**, 1800 (1998).

[9] I. Souza, T. Wilkens, and R. M. Martin, Polarization and localization in insulators: Generating function approach, Phys. Rev. B **62**, 1666 (2000).

[10] R. Resta and S. Sorella, Electron localization in the insulating state, Phys. Rev. Lett. **82**, 370 (1999).

[11] W. Kohn, Theory of the insulating state, Phys. Rev. **133**, A171 (1964).

[12] B. A. Bernevig and T. L. Hughes, *Topological Insulators and Superconductors* (Princeton University Press, Princeton, NJ, USA, 2013).

[13] J. K. Asbóth, L. Oroszlány, and A. Pályi, *A Short Course on Topological Insulators: Band Structure and Edge States in One and Two Dimensions*, Lecture Notes on Physica (Springer International Publishing, Berlin, Germany, 2016), Vol. 919.

[14] N. Marzari and D. Vanderbilt, Maximally localized generalized Wannier functions for composite energy bands, Phys. Rev. B **56**, 12847 (1997).

[15] N. Marzari, A. A. Mostofi, J. R. Yates, I. Souza, D. Vanderbilt, Maximally localized Wannier functions: Theory and applications, Rev. Mod. Phys. **84**, 1419 (2012).

[16] J. L. Cardy, *Scaling and Renormalization in Statistical Physics* (Cambridge Lecture Notes in Physics, Cambridge University Press, Cambridge, UK, 1996).

[17] M. E. Fisher, Critical phenomena, in *Proceedings of 51st Enrico Fermi Summer School*, Varena, edited by M. S. Green (Academic Press, NY, 1972).

[18] M. E. Fisher and M. N. Barber, Scaling theory for finite-size effects in the critical region, Phys. Rev. Lett. **28**, 1516 (1972).

[19] K. Binder, Finite size scaling analysis of Ising model block distribution functions, Z. Phys. B **43**, 119 (1981).

[20] K. Binder, Critical properties from Monte Carlo coarse graining and renormalization, Phys. Rev. Lett. **47**, 693 (1981).

[21] J. J. Shynk, *Probability, Random Variables and Random Processes: Theory and Signal Processing Applications* (John Wiley and Sons, Inc., Hoboken, NJ, 2013).

[22] E. Abrahams, P. W. Anderson, D. C. Licciardello, and T. V. Ramakrishnan, Scaling theory of localization, Phys. Rev. Lett. **42**, 673 (1979).

[23] A. Langedijk, B. van Tiggelen, and D. S. Wiersma, Fifty years of Anderson localization, Phys. Today **62**, 24 (2009).

[24] D. M. Basko, I. L. Aleiner, and B. L. Altshuler, Metal–insulator transition in a weakly interacting many-electron system with localized single-particle states, Ann. Phys. **321**, 1126 (2006).

[25] R. Nandkishore, D. A. Huse, Many-body localization and thermalization in quantum statistical mechanics, Annu. Rev. Condens. Matter Phys. **6**, 15 (2015).

[26] V. K. Varma and S. Pilati, Kohn's localization in disordered fermionic systems with and without interactions, Phys. Rev. B **92**, 134207 (2015).

[27] B. Hetényi and B. Dóra, Quantum phase transitions from analysis of the polarization amplitude, Phys. Rev. B **99**, 085126 (2019).

[28] B. Hetényi and S. Cengiz, Geometric cumulants associated with adiabatic cycles crossing degeneracy points: Application to finite size scaling of metal-insulator transitions in crystalline electronic systems, Phys. Rev. B **106**, 195151 (2022).

[29] S. Aubry and G. André, Analyticity breaking and Anderson localization in incommensurate lattices, Ann. Isr. Phys. Soc. **3**, 18 (1980).

[30] A. J. Martinez, M. A. Porter, and P. G. Kevrekidis, Quasiperiodic granular chains and Hofstadter butterflies, Philos. Trans. A **376**, 20170139 (2018).

[31] J. Billy, V. Josse, Z. Zuo, A. Bernard, B. Hambrecht, P. Logan, D. Clément, L. Sanchez-Palencia, P. Bouyer, and A. Aspect, Direct observation of Anderson localization of matter waves in a controlled disorder, Nature (London) **453**, 891 (2008).

[32] G. Roati, C. D'Errico, L. Fallani, M. Fattori, C. Fort, M. Zaccanti, G. Modugno, M. Modugno, and M. Inguscio, Anderson localization of a non-interacting Bose–Einstein condensate, Nature (London) **453**, 895 (2008).

[33] G. A. Domínguez-Castro and R. Paredes, The Aubry–André model as a hobbyhorse for understanding the localization phenomenon, Eur. J. Phys. **40**, 045403 (2019).

[34] S. Ya. Jitomirskaya, Metal-insulator transition for the almost Mathieu operator, Ann. Math. **150**, 1159 (1999).

[35] M. Modugno, Exponential localization in one-dimensional quasi-periodic optical lattices, New J. Phys. **11**, 033023 (2009).

[36] Y. Wang, G. Xianlong, and S. Chen, Almost mobility edges and the existence of critical regions in one-dimensional quasiperiodic lattices, Eur. Phys. J. B **90**, 215 (2017).

[37] Y. Zhang, D. Bulmash, A. V. Maharaj, C.-M. Jian, and S. A. Kivelson, The almost mobility edge in the almost Mathieu equation, arXiv:1504.05205.

[38] H. Rinne, *Location-Scale Distributions: Linear Estimation and Probability Plotting Using Matlab* (Justus-Liebig University Publications, Giessen, Germany, 2010).

[39] In lattice models, there is a contribution to the polarization from the nuclei, which shifts the average of the polarization of the electrons. In this work we are considering centered moments and cumulants which are unaffected by this shift.

[40] F. B. Hildebrand, *Finite-Difference Equations and Simulations* (Prentice-Hall, Englewood Cliffs, NJ, 1968).

[41] B. Hetényi, S. Parlak, and M. Yahyavi, Scaling and renormalization in the modern theory of polarization: Application to disordered systems, Phys. Rev. B **104**, 214207 (2021).

[42] C. N. Yang and C. P. Yang, One-dimensional chain of anisotropic spin-spin interactions. I. Proof of bethe's hypothesis for ground state in a finite system, Phys. Rev. **150**, 321 (1966).

[43] M. Thamm, H. Radhakrishnan, H. Barghathi, B. Rosenow, and A. Del Maestro, One-particle entanglement for one-dimensional spinless fermions after an interaction quantum quench, Phys. Rev. B **106**, 165116 (2022).

[44] P. Fazekas, The definition of the momentum density can be found in Chapter 10, *Lecture Notes on Electron Correlation and Magnetism* (World Scientific, Singapore 1999).

[45] G. Chiappe, E. Louis, and J. A. Vergés, Size-scaling behaviour of the electronic polarizability of one-dimensional interacting systems, J. Phys.: Condens. Matter **30**, 175603 (2018).